Performance of Optimum Switching Adaptive M-QAM for Amplify-and-Forward Relays

Tyler Nechiporenko, *Student Member, IEEE*, Prasanna Kalansuriya, *Student Member, IEEE*, and Chintha Tellambura, *Senior Member, IEEE*

***Abstract*—Optimization of the switching thresholds for constant-power adaptive five-mode M-ary quadrature amplitude modulation (M-QAM) transmission with an amplify-and-forward (AF) relay network is developed. The optimization criterion is the maximization of spectral efficiency subject to an average bit-error-rate (BER) constraint. This approach results in a constant-BER variable-rate M-QAM AF relay system, which requires feedback of $\log_2(N)$ bits for N modes. The performance analysis is based on an upper bound on the total effective SNR. Expressions are derived for the outage probability, the achievable spectral efficiency, and the error-rate performance for the AF cooperative system over both independent identically distributed (i.i.d.) and non-i.i.d. Rayleigh fading environments. The tightness of the upper bound is validated by Monte Carlo simulation. Adaptive five-mode M-QAM with optimum switching levels is shown to offer performance gains of 2–2.5 dB compared with fixed switching in terms of the transmit SNR to achieve specific spectral efficiency. Furthermore, the spectral efficiency of adaptive five-mode M-QAM with optimized switching comes within ∼6 dB of the theoretical Shannon channel capacity. However, this performance gain, which is obtained by employing adaptive M-QAM under cooperative diversity, comes at the cost of increased system complexity that is incurred due to the additional complexity of transmitter and receiver design.**

***Index Terms*—Adaptive transmission, amplify and forward (AF), Rayleigh fading.**

I. Introduction

ADAPTIVE transmission techniques have been extensively studied in conjunction with classical (i.e., noncooperative) communication networks. Adaptation effectively exploits the time-varying wireless channel by transmitting at higher speeds and/or higher power under favorable channel conditions and reduced speeds and/or power under poor channel conditions [1]–[5]. For instance, the transmitted power level, the symbol rate, the constellation size, the coding rate/scheme, or any combination of these parameters can be adjusted in response to the changing channel conditions [1]–[5]. Such transmitter adaptations in response to signal fading result in higher throughput and better utilization of the channel capacity. For example, adaptive M-ary quadrature amplitude modulation (M-QAM) schemes can achieve gains up to 20 dB over nonadaptive transmission [1].

Cooperative diversity utilizes a collection of distributed antennas belonging to multiple users in a network to combat the effects of fading [6], [7]. Although there has been extensive research on cooperative networks (e.g., see [8]–[15] for performance analysis of nonadaptive cooperative networks), the use of adaptive transmission techniques in cooperative networks has not received much attention. Current IEEE 802.16e systems use adaptive modulation, and the developing IEEE 802.16j standard specifies the use of cooperative diversity schemes. Hence, by integrating these two techniques, systems would be able to benefit from adaptive modulation and node cooperation [16], [17].

Moreover, it is to be noted that this form of adaptation is distinct from the conventional resource allocation problems. For example, resource allocation in terms of power and bandwidth for cooperative networks is investigated in [18]–[24]. These publications tend to focus on power-allocation problems, which are formulated by placing a fixed power constraint among the relays and allocating power to different nodes to optimize a performance objective. This requires the channel state information of all the links and fixed source rates, and, as a consequence, it is distinctly different from the adaptive policies that were considered in [1]–[5]. In general, the power-allocation problem has a high overhead when the number of nodes in the network is large. Furthermore, the rate adaptation at the transmitter is not considered in the above publications.

Previous Results: Since a large body of work exists on the performance analysis of (noncooperative) adaptive transmission techniques, only a brief survey is possible here. Several adaptive transmission techniques are analyzed in [1], [3], and [4] for single-antenna systems over Rayleigh and Nakagami fading channels, focusing on spectral efficiency and error-rate performance. In [2], the analysis in [1] and [3] is extended for diversity reception with multiple receive antennas. The work in [2] is extended to correlated Rayleigh fading in [5]. Moreover, it is shown in [25] for the traditional point-to-point links with adaptive M-QAM that the spectral efficiency can be increased by optimizing the switching thresholds when compared with fixed-switching thresholds.

In contrast, the performance analysis of adaptive cooperative networks has received much less attention. In [26], adaptive

Manuscript received June 20, 2008; revised September 6, 2008 and November 5, 2008. First published December 2, 2008; current version published May 11, 2009. T. Nechiporenko was supported in part by the Natural Sciences and Engineering Research Council of Canada (NSERC) Undergraduate Student Research Awards, by the NSERC Canada Graduate Scholarship, and by the iCORE Graduate Student Scholarship. The review of this paper was coordinated by Prof. S. Cui.

The authors are with the Department of Electrical and Computer Engineering, University of Alberta, Edmonton, AB T6G 2V4, Canada (e-mail: nechipor@ece.ualberta.ca; kalansur@ece.ualberta.ca; chintha@ece.ualberta.ca).

Color versions of one or more of the figures in this paper are available online at http://ieeexplore.ieee.org.

Digital Object Identifier 10.1109/TVT.2008.2010217

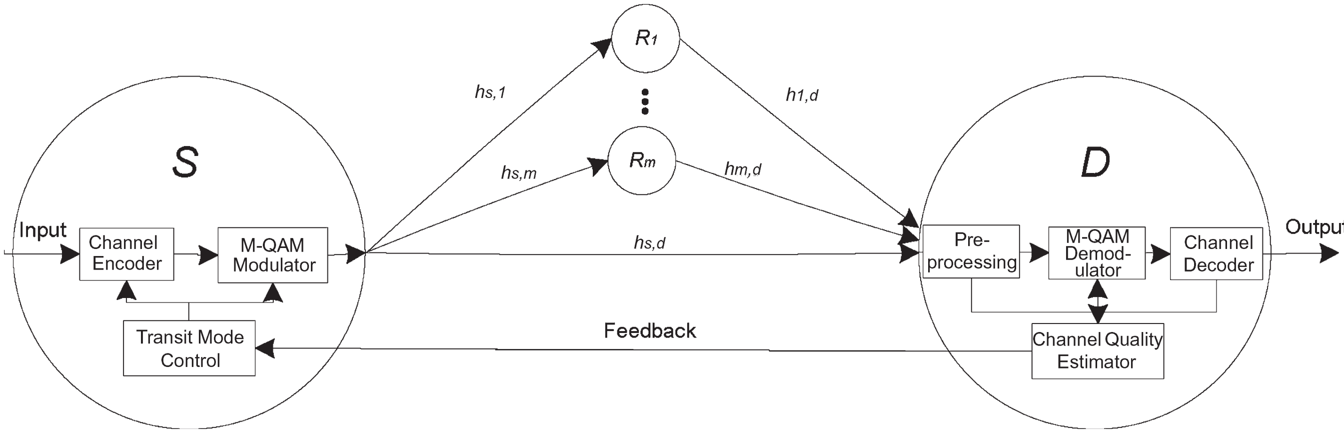

Fig. 1. Cooperative diversity wireless network with adaptive transmission.

transmission for a single relay (regenerative and nonregenerative) network without the direct path transmission is developed, and the capacity for the Rayleigh fading case is derived. More recently, Nechiporenko *et al.* [27] have proposed the use of adaptive transmission with an amplify-and-forward (AF) cooperative $m \geq 1$ relay network. Three different adaptive techniques are considered: 1) optimal simultaneous power and rate adaptation; 2) constant power with optimal rate adaptation; and 3) channel inversion with a fixed rate. The closed-form expressions are derived for the capacity of AF relaying over both independent identically distributed (i.i.d.) and non-i.i.d. Rayleigh fading environments under these adaptive techniques. The capacity analysis is based on an upper bound on the total effective SNR at the destination. In [28], the practical technique of adaptive M-QAM with fixed-switching thresholds is applied to the cooperative network in [27]. Simultaneously with the work in [27] and [28], Hwang *et al.* [29] derived the performance analysis of adaptive M-QAM for a single incremental AF relay in Nakagami fading. In [29], the same upper bound on the SNR that was used in [27] and [28] is considered, and the spectral efficiency, the bit error rate (BER), and the outage probability are found.

Our Contributions: Motivated by these observations, this paper optimizes the switching thresholds for constant-power[1] adaptive five-mode M-QAM transmission over an AF relay link. The optimization is based on the 1-D Lagrangian optimization method that was developed in [25]. The switching thresholds are optimized to maximize the spectral efficiency such that an average BER constraint is satisfied. We compare the performance of optimal switching thresholds to that of fixed-switching thresholds where an instantaneous BER constraint is enforced. The closed-form expressions for the outage probability, the achievable spectral efficiency, and the BER for the AF cooperative network in i.i.d. and non-i.i.d. Rayleigh fading environments are computed and compared. Note that these results provide a different perspective on the system implementation and analysis from our previous results [27], where the Shannon capacity for the nonregenerative cooperative system under adaptive transmission for i.i.d. and non-i.i.d. Rayleigh fading channels is derived. Furthermore, the results of this paper are a more complete analysis of our initial findings that were published in [28], where adaptive M-QAM with fixed switching is only considered.

This paper is organized as follows. Section II presents the channel and system model. The analysis of adaptive M-QAM is conducted in Section III. In Section IV, the optimization of the switching thresholds is discussed. The numerical results are presented in Section V. Conclusions are given in Section VI.

II. Channel and System Model

A. System Model

In the cooperative wireless network of Fig. 1, a source node S communicates with a destination node D via a direct link and through m AF relays R_i, $i \in \{1, 2, \ldots, m\}$. Communication occurs in two phases. In the first phase, the source transmits signal x to the destination and the relays. The received signals at the destination and at the ith relay are respectively given by

$$r_{s,d} = h_{s,d}x + n_{s,d} \tag{1}$$
$$r_{s,i} = h_{s,i}x + n_{s,i}, \qquad i = 1, \ldots, m \tag{2}$$

where $h_{s,i}$, $h_{i,d}$, and $h_{s,d}$ denote the Rayleigh fading channel coefficients between the source and the ith relay, the ith relay and the destination, and the source and the destination, respectively. The additive white Gaussian noise (AWGN) is denoted at the relays as $n_{s,i}$ and at the destination as $n_{s,d}$ and $n_{i,d}$.

The ith relay amplifies the received signal and transmits it to the destination in the second phase of cooperation. During the second phase, the m relays use m orthogonal channels. Without lost of generality, this can be accomplished by using time-division multiple access [7]. That is, each of the m symbols is transmitted from the relays in a round-robin fashion. The received signal at the destination from the ith relay is

$$r_{i,d} = G_i h_{i,d} r_{s,i} + n_{i,d}, \qquad i = 1, \ldots, m \tag{3}$$

where G_i is the ith relay amplifier gain, chosen as in [7]. $G_i^2 = E_s/(E_s|h_{s,i}|^2 + N_0)$, where E_s is the average symbol energy, and N_0 is the noise variance.

[1] Adaptive schemes can also have variable power. In this paper, we focus only on constant power, as it has been shown that the gain in the spectral efficiency that is achieved by variable-power schemes over the constant-power schemes is marginal [1], [3], [4], [25].

Using maximum-ratio combining at the destination node, the total SNR is easily found as [7]

$$\gamma_{\text{tot}} = \gamma_{s,d} + \sum_{i=1}^{m} \frac{\gamma_{s,i}\gamma_{i,d}}{\gamma_{s,i}+\gamma_{i,d}+1} \tag{4}$$

where $\gamma_{s,i} = |h_{s,i}|^2 E_s/N_0$, $\gamma_{i,d} = |h_{i,d}|^2 E_s/N_0$, and $\gamma_{s,d} = |h_{s,d}|^2 E_s/N_0$ are the instantaneous SNRs between S and R_i, R_i and D, and S and D, respectively.

An upper bound of the total SNR at the destination node can be found as [9], [30]

$$\gamma_{\text{tot}} \leq \gamma_{s,d} + \sum_{i=1}^{m} \gamma_i = \gamma_{\text{ub}} \tag{5}$$

where $\gamma_i = \min(\gamma_{s,i}, \gamma_{i,d})$. Note that we do not try to derive the probability density function (pdf) of the exact SNR [see (4)]. The main reason is that it is extremely complicated to obtain. Our subsequent analysis exclusively relies on γ_{ub}; we provide extensive simulation results in Section V to complement the bounds. A lower bound can be formulated as in [30], where $\gamma_i = 0.5\min(\gamma_{s,i}, \gamma_{i,d})$. As the lower bound is different from the upper bound only by a factor of one half, the following analysis can easily be extended to the lower bound, but is omitted for brevity. Furthermore, we have chosen to exclude plotting the lower bound in Section V to reduce the clutter of the figures. However, see [27] for accuracy regarding the bounds.

B. PDF

Note that we focus on the Rayleigh fading model to keep the analysis as simple as possible. This paper can be extended to the more general Nakagami fading model; however, this is not attempted here. For brevity, we omit the derivations and simply use the results from [27]. To proceed further, we consider two different cases of fading channel statistics as follows.

1) I.I.D. Rayleigh Fading Channels: In [27], the pdf for i.i.d. Rayleigh fading using the bound of (5) is given as

$$p_{\gamma_{\text{ub}}}(\gamma) = \frac{\beta_0}{\bar{\gamma}_{s,d}} e^{-\frac{\gamma}{\bar{\gamma}_{s,d}}} + \sum_{i=1}^{m} \frac{\beta_i (0.5\bar{\gamma})^{-i}}{(i-1)!} \gamma^{i-1} e^{-\frac{\gamma}{(0.5\bar{\gamma})}} \tag{6}$$

where $\bar{\gamma} = \mathbf{E}\{|h_{s,i}|^2\}E_s/N_0 = \mathbf{E}\{|h_{i,d}|^2\}E_s/N_0$, and

$$\beta_0 = \left(1 - \frac{\bar{\gamma}}{2\bar{\gamma}_{s,d}}\right)^{-m}$$
$$\beta_i = \frac{(0.5\bar{\gamma})^{(i-m)}}{(m-i)!} \frac{\partial^{m-i}}{\partial s^{m-i}} \left[(1+\bar{\gamma}_{s,d}s)^{-1}\right]_{s=-1/(0.5\bar{\gamma})}. \tag{7}$$

2) Non-I.I.D. Rayleigh Fading Channels: In practice, the relays are often not placed symmetrically, which causes different fading statistics among the relay–destination links. Thus, it makes sense to consider the non-i.i.d. case. Similar to the case of i.i.d. fading, the pdf is given in [27] as

$$p_{\gamma_{\text{ub}}}(\gamma) = \frac{\widehat{\beta}_0}{\bar{\gamma}_{s,d}} e^{-\frac{\gamma}{\bar{\gamma}_{s,d}}} + \sum_{i=1}^{m} \frac{\widehat{\beta}_i}{\tau_i} e^{-\frac{\gamma}{\tau_i}} \tag{8}$$

where $\tau_i = (\bar{\gamma}_{s,i}\bar{\gamma}_{i,d})/(\bar{\gamma}_{s,i}+\bar{\gamma}_{i,d})$, $\bar{\gamma}_{s,i} = \mathbf{E}\{|h_{s,i}|^2\}E_s/N_0$, $\bar{\gamma}_{i,d} = \mathbf{E}\{|h_{i,d}|^2\}E_s/N_0$, and

$$\widehat{\beta}_0 = \prod_{i=1}^{m}\left(1 - \frac{\tau_i}{\bar{\gamma}_{s,d}}\right)^{-1}$$
$$\widehat{\beta}_i = \left(1 - \frac{\bar{\gamma}_{s,d}}{\tau_i}\right)^{-1} \prod_{k=1,k\neq i}^{m} \left(1 - \frac{\tau_k}{\tau_i}\right)^{-1}, \qquad i = 1, \ldots, m. \tag{9}$$

III. ADAPTIVE M-QAM

In this section, the analysis for adaptive discrete rate (ADR) M-QAM is developed. The technique of ADR M-QAM is first explained followed by the outage probability, the spectral efficiency, and the BER analysis. The outage probability and the spectral efficiency are derived for an arbitrary number of switching regions. We then focus on the five-mode M-QAM system for the BER analysis.

A. ADR Modulation

Adaptive rate modulation has several practical advantages. The destination needs only to calculate the total SNR, select the appropriate transmission rate, and send this information back to the transmitter. For an N-mode adaptive scheme, at least $\log_2(N)$ bits of feedback information from the destination is required for proper rate selection at the transmitter. This makes adaptive techniques based on adaptive M-QAM such as those proposed in [3] and [4] viable. For this reason, adaptive M-QAM is also considered in this paper as a practical extension to the theoretical work in [27].

The ADR M-QAM scheme performs as follows. The range of the effective received SNR is divided into $N+1$ regions, partitioned by a set of switching thresholds. In each region, a specific constellation of size M_n is used. Due to signal fading, the effective SNR falls into the nth region $(n = 0, 1, \ldots, N)$, and the constellation of size M_n is used for transmission. In this paper, although the case of general N-mode M-QAM can be treated, for reasons of brevity and simplicity, we limit our study to five-mode adaptive M-QAM. Moreover, this case has been well studied [3], [25], [31], [32]. The parameters for five-mode adaptive M-QAM are given in Table I, where, again, γ is the instantaneous received SNR, b_n is the number of bits per a transmitted symbol, $\gamma_0 = 0$, and $\gamma_5 = \infty$.

B. Outage Probability

1) Case of I.I.D. Fading Channels: As no transmission occurs when the received SNR is below the smallest predetermined switching level γ_1, the probability of such an outage event is given by

$$P_{\text{out}} = P[\gamma_{\text{ub}} < \gamma_1] = \int_0^{\gamma_1} p_{\gamma_{\text{ub}}}(\gamma)d\gamma$$
$$= 1 - \int_{\gamma_1}^{\infty} p_{\gamma_{\text{ub}}}(\gamma)d\gamma \tag{10}$$

TABLE I
FIVE-MODE ADAPTIVE M-QAM PARAMETERS

SNR	$\gamma_0 \le \gamma < \gamma_1$	$\gamma_1 \le \gamma < \gamma_2$	$\gamma_2 \le \gamma < \gamma_3$	$\gamma_3 \le \gamma < \gamma_4$	$\gamma_4 \le \gamma < \gamma_5$
n	0	1	2	3	4
M_n	0	2	4	16	64
b_n	0	1	2	4	6
mode	No Tx	BPSK	QPSK	16-QAM	64-QAM

where

$$\int_{\gamma_1}^{\infty} p_{\gamma_{\rm ub}}(\gamma)d\gamma = \beta_0 e^{-\frac{\gamma_1}{\bar{\gamma}_{s,d}}} + e^{-\frac{2\gamma_1}{\bar{\gamma}}} \sum_{i=1}^{m} \beta_i \sum_{k=0}^{i-1} \frac{1}{k!}\left(\frac{2\gamma_1}{\bar{\gamma}}\right)^k \tag{11}$$

is established by using [33, eq. (3.351.2)].

The probability of outage is found by substituting (11) into (10), resulting in

$$P_{\rm out} = 1 - \left[\beta_0 e^{-\frac{\gamma_1}{\bar{\gamma}_{s,d}}} + e^{-\frac{2\gamma_1}{\bar{\gamma}}} \sum_{i=1}^{m} \beta_i \sum_{k=0}^{i-1} \frac{1}{k!}\left(\frac{2\gamma_1}{\bar{\gamma}}\right)^k\right]. \tag{12}$$

2) Case of Non-I.I.D. Fading Channels: In a similar fashion as the i.i.d. case, the tail probability is given by

$$\int_{\gamma_1}^{\infty} p_{\gamma_{\rm ub}}(\gamma)d\gamma = \widehat{\beta}_0 e^{-\frac{\gamma_1}{\bar{\gamma}_{s,d}}} + \sum_{i=1}^{m} \widehat{\beta}_i e^{-\frac{\gamma_1}{\tau_i}}. \tag{13}$$

Likewise, the probability of outage is found by substituting (13) into (10) to give

$$P_{\rm out} = 1 - \left[\widehat{\beta}_0 e^{-\frac{\gamma_1}{\bar{\gamma}_{s,d}}} + \sum_{i=1}^{m} \widehat{\beta}_i e^{-\frac{\gamma_1}{\tau_i}}\right]. \tag{14}$$

C. Achievable Spectral Efficiency

1) Case of I.I.D. Fading Channels: For ADR M-QAM, the achievable average spectral efficiency is simply the sum of the data rates in each of the partition regions weighted by the probability of occurrence of each region and is given as follows:

$$R_{\rm adr} = \frac{B}{(m+1)} \sum_{n=1}^{N} b_n \delta_n \tag{15}$$

where $b_n = \log_2(M_n)$ corresponds to the data rate of the nth region, and B is the bandwidth. The factor $1/(m+1)$ accounts for the fact that the transmission process takes place in $(m+1)$ orthogonal channels or timeslots. Furthermore, δ_n is the probability that the effective received SNR is in the nth partition region and is given as

$$\delta_n = \int_{\gamma_n}^{\gamma_{n+1}} p_{\gamma_{\rm ub}}(\gamma)d\gamma \tag{16}$$

which evaluates to

$$\delta_n = \beta_0\left(e^{-\gamma_n/\gamma_{s,d}} - e^{-\gamma_{n+1}/\gamma_{s,d}}\right) + \sum_{i=1}^{m} \beta_i \left(e^{-\frac{2\gamma_n}{\bar{\gamma}}} \sum_{j=1}^{i-1} \frac{\left(\frac{2\gamma_n}{\bar{\gamma}}\right)^j}{j!} - e^{-\frac{2\gamma_{n+1}}{\bar{\gamma}}} \sum_{j=1}^{i-1} \frac{\left(\frac{2\gamma_{n+1}}{\bar{\gamma}}\right)^j}{j!} \right). \tag{17}$$

TABLE II
M-QAM BER PARAMETERS

M_n	Mode	$\{(A_l, a_l)\}$
2	BPSK	$\{(1,2)\}$
4	QPSK	$\{(1,1)\}$
16	16-QAM	$\left\{(\frac{3}{4},\frac{1^2}{5}),(\frac{2}{4},\frac{3^2}{5}),(-\frac{1}{4},\frac{5^2}{5})\right\}$
64	64-QAM	$\left\{(\frac{7}{12},\frac{1^2}{21}),(\frac{6}{12},\frac{3^2}{21}),(-\frac{1}{12},\frac{5^2}{21}),(\frac{1}{12},\frac{9^2}{21}),(-\frac{1}{12},\frac{13^2}{21})\right\}$

2) Case of Non-I.I.D. Fading Channels: In a similar manner to the i.i.d. fading channel, the average ADR M-QAM spectral efficiency is $R_{\rm adr}$ for the non-i.i.d. fading channel, which can be found by using (15), where δ_n is given by

$$\delta_n = \widehat{\beta}_0\left(e^{-\gamma_n/\gamma_{s,d}} - e^{-\gamma_{n+1}/\gamma_{s,d}}\right) + \sum_{i=1}^{m} \widehat{\beta}_i\left(e^{-\gamma_n/\tau_i} - e^{-\gamma_{n+1}/\tau_i}\right). \tag{18}$$

D. Average BER

1) Case of I.I.D. Fading Channels: For ADR M-QAM, the average $\text{BER}_{\rm adr}$ can easily be calculated, as it is simply the ratio of the average number of bits in error divided by the total average number of transmitted bits [4], [25], i.e.,

$$\text{BER}_{\rm adr} = \frac{\sum_{n=1}^{N} b_n P_{n,\rm QAM}}{\sum_{n=1}^{N} b_n \delta_n} \tag{19}$$

where $P_{n,\rm QAM}$ is the average BER in a specific SNR region of $[\gamma_n, \gamma_{n+1}]$ and can be represented as

$$P_{n,\rm QAM} = \int_{\gamma_n}^{\gamma_{n+1}} p_{m_n,\rm QAM}(\gamma) p_{\gamma_{\rm ub}}(\gamma)d\gamma \tag{20}$$

where $p_{m_n,\rm QAM}(\gamma)$ is the BER of a system, which implements square M-QAM over an AWGN channel, with coherent detection and Gray coding as in [25], i.e.,

$$p_{m_n,\rm QAM}(\gamma) = \sum_{l} A_l Q\left(\sqrt{a_l \gamma}\right) \tag{21}$$

where $Q(\cdot)$ is the standard Gaussian Q-function defined as $Q(x) = (1/\sqrt{2\pi})\int_x^{\infty} \exp(-\lambda^2/2)d\lambda$, γ is the received SNR, and A_l and a_l are some constants shown in Table II.

After some mathematical manipulations, as shown in the Appendix, $P_{n,\rm QAM}$ can be written as in (22), shown at the bottom of the next page.

Since the error-rate expression in (21) can be used to represent the BER of M-ary phase-shift keying (MPSK) as well [25], our derivations can also be extended to adaptive MPSK schemes.

2) Case of Non-I.I.D. Fading Channels: In a similar manner to the i.i.d. fading channel, the average BER can be computed as in (19), where

$$\begin{aligned}
P_{n,\mathrm{QAM}} = \widehat{\beta}_0 \sum_l A_l \Bigg[& Q(\sqrt{a_l\gamma})\Big[1-e^{-\frac{\gamma}{\bar{\gamma}_{s,d}}}\Big]\Big|_{\gamma_n}^{\gamma_{n+1}} \\
& -\frac{1}{2}\Bigg\{(\pi)^{-0.5}\Gamma\Big(0.5,\frac{\gamma a_l}{2}\Big)\Big|_{\gamma_n}^{\gamma_{n+1}} \\
& -\sqrt{\frac{a_l}{2\pi}}\left(a_l/2+\bar{\gamma}_{s,d}^{-1}\right)^{-0.5} \\
& \times\Gamma\Big(0.5,\big(a_l/2+\bar{\gamma}_{s,d}^{-1}\big)\gamma\Big)\Big|_{\gamma_n}^{\gamma_{n+1}}\Bigg\}\Bigg] \\
+\sum_l A_l \sum_{i=1}^{m}\widehat{\beta}_i & \\
\times\Bigg[& Q(\sqrt{a_l\gamma})\Big[1-e^{-\frac{\gamma}{\tau_i}}\Big]\Big|_{\gamma_n}^{\gamma_{n+1}} \\
& -\frac{1}{2}\Bigg\{(\pi)^{-0.5}\Gamma\Big(0.5,\frac{\gamma a_l}{2}\Big)\Big|_{\gamma_n}^{\gamma_{n+1}} \\
& -\sqrt{\frac{a_l}{2\pi}}\left(a_l/2+\tau_i^{-1}\right)^{-0.5} \\
& \times\Gamma\big(0.5,(a_l/2+\tau_i^{-1})\gamma\big)\Big|_{\gamma_n}^{\gamma_{n+1}}\Bigg\}\Bigg]. \qquad (23)
\end{aligned}$$

IV. Switching Thresholds

A. Fixed-Switching Thresholds

With fixed partitioning, to have the reliable communication achieve a specific BER target of BER_0 using M_n-QAM, the switching thresholds or region boundaries are set to the SNR that is required to achieve this desired performance [4], i.e.,

$$\begin{aligned}
\gamma_0 &= 0 \\
\gamma_1 &= \left[\mathrm{erfc}^{-1}(2\mathrm{BER}_0)\right]^2 \\
\gamma_n &= \frac{2}{3}K_0(M_n-1), \qquad n=2,3,\ldots,N \\
\gamma_{N+1} &= +\infty \qquad (24)
\end{aligned}$$

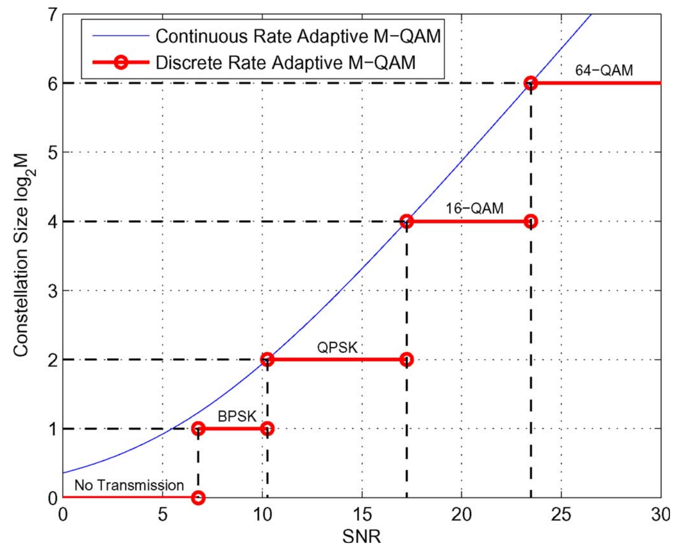

Fig. 2. Constellation size relative to the received SNR (in decibels).

where $\mathrm{erfc}^{-1}(\cdot)$ is the inverse complementary error function, and $K_0 = -\ln(5\mathrm{BER}_0)$. This partition of the switching thresholds is shown in Fig. 2 for five-mode adaptive M-QAM for a desired BER_0 of 10^{-3}. However, this technique only limits the peak instantaneous BER and is an inefficient use of a spectrum or, in other words, results in lower spectral efficiency. It will be shown next that the switching thresholds can be optimized so that the average BER always meets the desired BER threshold.

B. Optimum Switching Thresholds

Subject to a constraint on the average BER, the switching thresholds can be optimized to maximize the throughput. For instance, in [4], the switching thresholds are chosen as in (24), which are designed for an AWGN channel. Optimization of the switching thresholds can be performed so that the average BER always meets the desired BER threshold. That is, one designs a set of switching thresholds, which is denoted as $\boldsymbol{s} = \{\gamma_n | n=0,1,\ldots,N\}$, such that average throughput $R_{\mathrm{adr}}(\bar{\gamma},\boldsymbol{s})$ is maximized under the constraint that the average BER is equal to the desired BER target, i.e., $\mathrm{BER}_{\mathrm{adr}} = \mathrm{BER}_0$. The Lagrangian optimization technique for deriving the globally

$$\begin{aligned}
P_{n,\mathrm{QAM}} = \beta_0 \sum_l A_l \Bigg[& Q\left(\sqrt{a_l\gamma}\right)\left[1-e^{-\frac{\gamma}{\bar{\gamma}_{s,d}}}\right]\Big|_{\gamma_n}^{\gamma_{n+1}} - \frac{1}{2}\Bigg\{(\pi)^{-0.5}\Gamma\left(0.5,\frac{\gamma a_l}{2}\right)\Big|_{\gamma_n}^{\gamma_{n+1}} - \sqrt{\frac{a_l}{2\pi}}\left(a_l/2+\bar{\gamma}_{s,d}^{-1}\right)^{-0.5} \\
& \times\Gamma\left(0.5,\left(a_l/2+\bar{\gamma}_{s,d}^{-1}\right)\gamma\right)\Big|_{\gamma_n}^{\gamma_{n+1}}\Bigg\}\Bigg] \\
+\sum_l A_l \sum_{i=1}^{m}\beta_i\Bigg[& Q\left(\sqrt{a_l\gamma}\right)\left(1-e^{-\frac{\gamma}{(0.5\bar{\gamma})}}\sum_{r=0}^{i-1}\frac{(2\gamma/\bar{\gamma})^r}{r!}\right)\Bigg|_{\gamma_n}^{\gamma_{n+1}} \\
& -\frac{1}{2}\Bigg\{(\pi)^{-0.5}\Gamma\left(0.5,\frac{\gamma a_l}{2}\right)\Big|_{\gamma_n}^{\gamma_{n+1}} - \sqrt{\frac{a_l}{2\pi}}\sum_{r=0}^{i-1}\frac{(0.5\bar{\gamma})^{-r}}{r!}(a_l/2+2/\bar{\gamma})^{-r-0.5} \\
& \times\Gamma\left(r+0.5,(a_l/2+2/\bar{\gamma})\gamma\right)\Big|_{\gamma_n}^{\gamma_{n+1}}\Bigg\}\Bigg] \qquad (22)
\end{aligned}$$

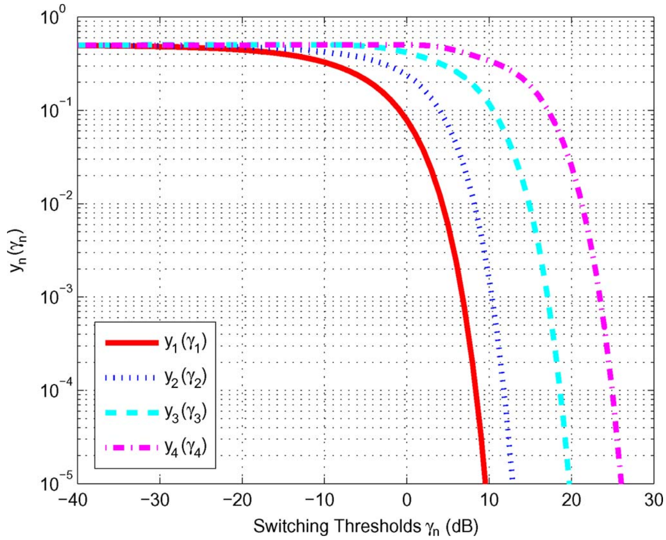

Fig. 3. Switching level constraint relationship.

optimized modulation-mode switching thresholds can then be used [25]. The optimization problem that is required is only 1-D and can be performed offline, so it does not add a layer of complexity to the system.

Lagrangian Optimization Problem Formulation: Maximize the *objective function* $R_{\rm adr}(\bar{\gamma}, \boldsymbol{s})$ as given in (15), which is *constrained* by $\text{BER}_{\rm adr} = \text{BER}_0$ as given in (19), i.e.,

$$\max_{\boldsymbol{s}} \sum_{n=1}^{N} b_n \delta_n \tag{25}$$

$$\text{subject to} \quad \sum_{n=1}^{N} b_n P_{n,\rm QAM} = \text{BER}_0 \sum_{n=1}^{N} b_n \delta_n. \tag{26}$$

Furthermore, assuming that the switching thresholds are ordered, i.e.,

$$\gamma_n \leq \gamma_{n+1} \tag{27}$$

and $\gamma_0 = 0$ and $\gamma_N = \infty$, the optimization problem consists of $N-1$ independent variables and, hence, is an $(N-1)$-dimensional optimization problem, as discussed in [25]. Using a modified objective function, it is shown in [25] that this problem can be formulated as a 1-D Lagrangian optimization problem. The details can be found in [25], and only the important results are summarized here.

The first step is to identify that γ_n $(n \geq 1)$ are all dependent on γ_1, and it is shown in [25] that, for five-mode adaptive M-QAM, the switching thresholds $\boldsymbol{s}$ are constrained by the following:

$$y_k(\gamma_k) = y_1(\gamma_1), \qquad \text{for } k = 2, 3, \ldots, N \tag{28}$$

$$y_1(\gamma_1) = p_{2,\rm QAM}(\gamma_1) \tag{29}$$

$$y_2(\gamma_2) = 2p_{4,\rm QAM}(\gamma_2) - p_{2,\rm QAM}(\gamma_2) \tag{30}$$

$$y_3(\gamma_3) = 2p_{16,\rm QAM}(\gamma_3) - p_{4,\rm QAM}(\gamma_3) \tag{31}$$

$$y_4(\gamma_4) = 3p_{64,\rm QAM}(\gamma_4) - 2p_{16,\rm QAM}(\gamma_4) \tag{32}$$

and are plotted in [25] and illustrated here for clarity in Fig. 3.

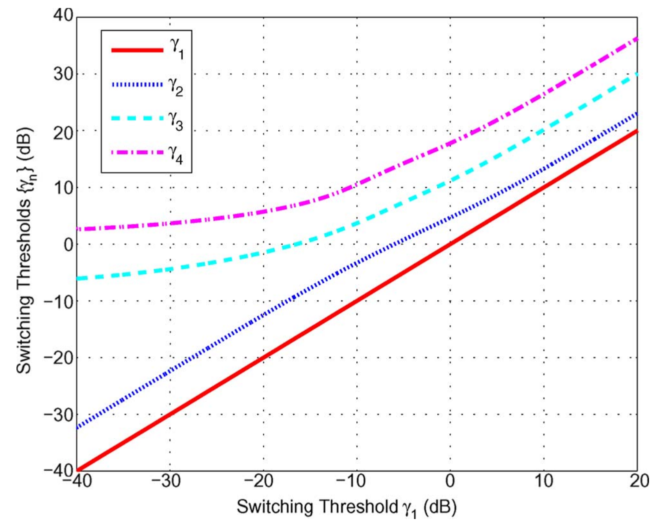

Fig. 4. Switching thresholds as a function of γ_1.

Given (28)–(32), the switching thresholds γ_2, γ_3, and γ_4 can be found in terms of γ_1. That is, $\gamma_2 = y_2^{-1}(y_1(\gamma_1))$, $\gamma_3 = y_3^{-1}(y_1(\gamma_1))$, and $\gamma_4 = y_4^{-1}(y_1(\gamma_1))$. The corresponding values of γ_2, γ_3, and γ_4 can numerically be found in terms of γ_1 and are provided in [25], but they are presented here for clarity in Fig. 4.

Since all the switching thresholds depend on the first threshold γ_1, the optimization problem is only concerned with finding the optimal value for γ_1. For a given target BER of BER_0, and the pdf of effective SNR (6) or (8), the optimal value for γ_1 can be solved. Thus, the optimization problem is a simple 1-D root-finding problem, where the constraint function is given as in [25], i.e.,

$$Y\left(\bar{\gamma}; \boldsymbol{s}(\gamma_1)\right) = \sum_{n=1}^{N} b_n P_{n,\rm QAM} - \text{BER}_0 \sum_{n=1}^{N} b_n \delta_n = 0. \tag{33}$$

Clearly, the relationship between (26) and $Y(\bar{\gamma}; \boldsymbol{s}(\gamma_1))$ in (33) is noticeable. Furthermore, the first term of $Y(\bar{\gamma}; \boldsymbol{s}(\gamma_1))$ can intuitively be thought of as the sum of the BER in each mode that is weighted by the average throughput of each mode [25]. On the other hand, the second term of $Y(\bar{\gamma}; \boldsymbol{s}(\gamma_1))$ is the average throughput that is weighted by the target BER threshold. This means that $Y(\bar{\gamma}; \boldsymbol{s}(\gamma_1))$ in (33) represents the difference between the average BER and the desired BER, i.e., BER_0. Consequently, the problem is finding the solution to $Y(\bar{\gamma}; \boldsymbol{s}(\gamma_1)) = 0$ when it exists.

V. Numerical Results and Comparisons

This section presents the numerical results for the achievable spectral efficiency, the outage probability, and the BER for cooperative systems with adaptive five-mode M-QAM transmission. Optimal switching thresholds and fixed-switching thresholds are computed and compared. For i.i.d. and non-i.i.d. Rayleigh fading, systems with one relay, i.e., $m = 1$, and two relays, i.e., $m = 2$, are considered, respectively. However, the results of Sections III and IV can be used for any number of relays.

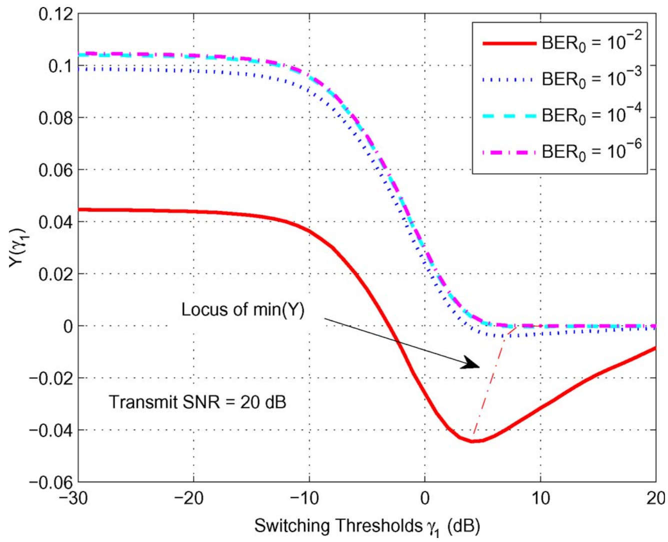

Fig. 5. Constraint function $Y(\bar{\gamma}; \boldsymbol{s}(\gamma_1))$ for i.i.d. Rayleigh fading with $m = 1$ relay.

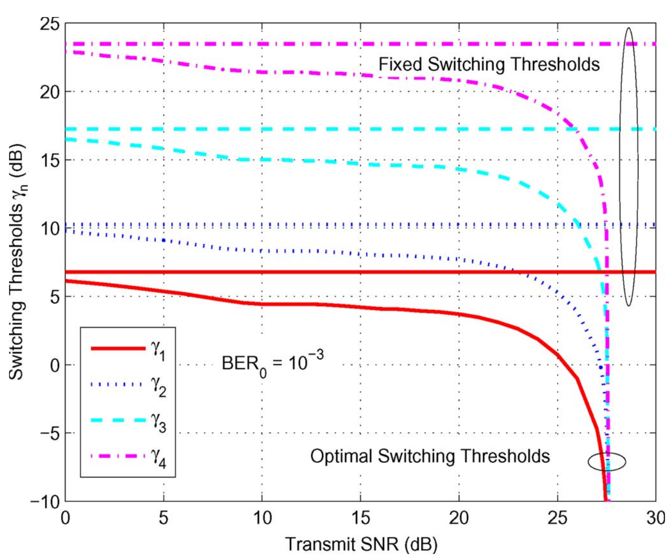

Fig. 6. Switching thresholds for i.i.d. Rayleigh fading with $m = 1$ relay.

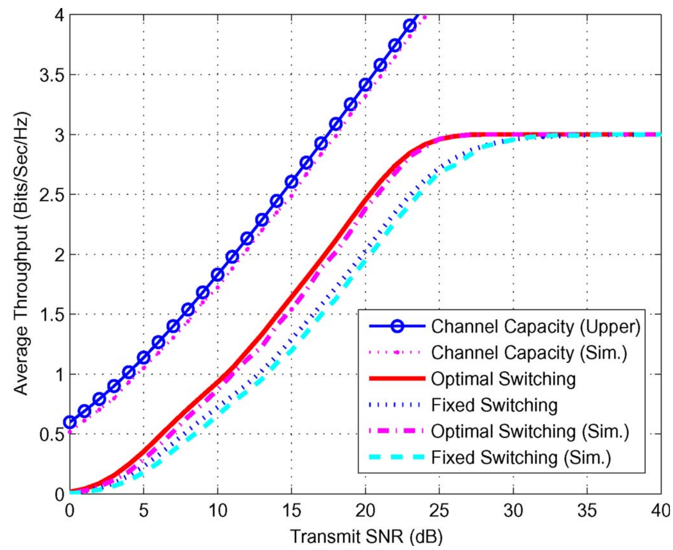

Fig. 7. Achievable rate for i.i.d. Rayleigh fading with $m = 1$ relay.

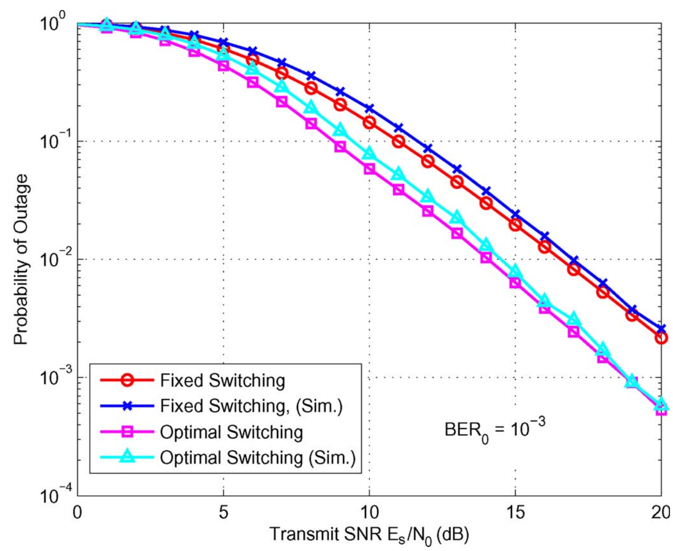

Fig. 8. Outage probability for i.i.d. Rayleigh fading with $m = 1$ relay.

In Fig. 5, constraint function (33) is plotted for i.i.d. Rayleigh fading with one relay, i.e., $m = 1$, where $\bar{\gamma}_{s,d} = \bar{\gamma}$. Adaptive five-mode M-QAM is considered where the average transmit SNR is set to 20 dB. $Y(\bar{\gamma}; \boldsymbol{s}(\gamma_1))$ is plotted for several target BER thresholds $\text{BER}_0 = \{10^{-2}, 10^{-3}, 10^{-4}, 10^{-6}\}$ to illustrate the solution to $Y(\bar{\gamma}; \boldsymbol{s}(\gamma_1)) = 0$.

Fig. 6 shows the switching thresholds for both the Lagrangian optimization technique and the fixed-switching thresholds as given in (24) for adaptive five-mode M-QAM for i.i.d. Rayleigh fading with one relay, where the target BER is set to $\text{BER}_0 = 10^{-3}$. It can be seen that there is an avalanche SNR of $\overline{\gamma}_a \sim 27.5$ dB, where all of the switching thresholds avalanche to zero. This occurs when the BER of the highest order modulation mode is equal to the target BER threshold, i.e., P_4, $\text{QAM}(\overline{\gamma}_a) = \text{BER}_0$. Once this avalanche SNR is reached, rate adaptation is abandoned, and only the highest order modulation mode is used for transmission. Furthermore, it is worth mentioning that a unique solution to (33), i.e., $Y(\bar{\gamma}; \boldsymbol{s}(\gamma_1)) = 0$, exists as long as the transmit SNR is less than the avalanche SNR, i.e., $\bar{\gamma} < \bar{\gamma}_a$.

For optimal switching and fixed switching, the achievable spectral efficiency is plotted in Fig. 7 for adaptive five-mode M-QAM for i.i.d. Rayleigh fading with one relay, where the target BER is set to $\text{BER}_0 = 10^{-3}$. Optimal switching compared to fixed switching results in an ∼2- to 2.5-dB gain of the required transmit SNR to achieve a specific average throughput. Monte Carlo simulation is also plotted along with the upper bound analysis. The upper bound is fairly tight and is within 1 dB of the simulation results; this is as expected, as similar results occur in [9], [27], [28], and [30]. Furthermore, in Fig. 8, the outage probability is plotted. Similarly, there is an improvement in the required transmit SNR for a specific outage probability. For instance, at a probability of outage of 10^{-2}, there is an ∼2-dB gain in the SNR. The BER is plotted in Fig. 9. It is clear that the optimal switching always meets the desired BER threshold of $\text{BER}_0 = 10^{-3}$ until the avalanche SNR is reached, where it then has the error probability that is

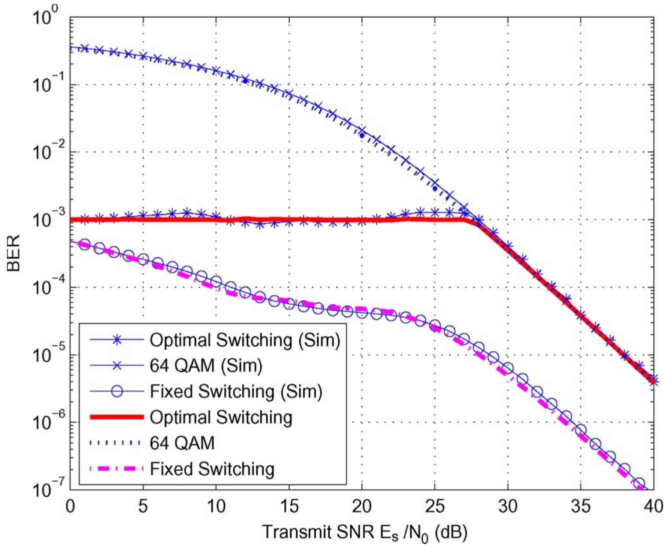

Fig. 9. Average BER for i.i.d. Rayleigh fading with $m = 1$ relay.

equal to the error probability for 64-QAM. Also, the BER for fixed switching results in a conservative average BER that is always below the BER target of $\text{BER}_0 = 10^{-3}$. Semianalytical simulation results for the BER are also plotted; that is, (21) is used to calculate the instantaneous BER, whereas the channel model is simulated statistically. The simulation results for the BER are fairly tight to the analytical results and further substantiate the validity of using the upper bound of (5). Note that the simulated BER values instantaneously deviate from the target BER and take higher values. This is because optimum switching levels that are analytically derived by solving (33) using the upper bound pdf were used in the simulation that was carried out using the statistically simulated exact pdf.

For non-i.i.d. Rayleigh fading, we have generated simulation and analytical results, which are not shown here for brevity. Results that are obtained for the outage probability, the achievable spectral efficiency, and the BER performance were similar to those of the i.i.d. case.

VI. Conclusion

This paper has investigated optimum switching and fixed-switching adaptive M-QAM schemes for i.i.d. and non-i.i.d. Rayleigh fading cooperative channels. The optimum thresholds have been derived to maximize the spectral efficiency subject to an average BER constraint using the Lagrangian optimization technique. The performance of optimum switching and fixed-switching adaptive M-QAM has been analyzed and compared. Specifically, the outage probability, the achievable spectral efficiency, and the BER have been derived. The analysis relied on using an upper bound on the effective received SNR [see (5)]. Monte Carlo simulation results show the accuracy regarding the performance of the effective received SNR bound. The results indicate that, for a specific average throughput, optimum switching thresholds gain 2.5 dB compared to fixed switching. Note, however, that this performance gain of cooperative ADR M-QAM comes at the cost of increased system complexity that is incurred due to the additional complexity of transmitter and receiver design. Moreover, an N-mode system requires feedback of $\log_2(N)$ bits from the destination to the source and relays. The spectral efficiency of adaptive five-mode M-QAM with optimized switching has been compared with the theoretical Shannon channel capacity derived in [27] and approaches this fundamental limit within ~6 dB. This paper can be extended in several ways. For instance, decode-and-forward relaying and other fading models can be considered. We are currently working on some of these problems.

Appendix

Case of I.I.D. Fading Channels: The BER for square QAM with gray coding over an AWGN channel can be represented as follows [25]:

$$p_{m_n,\text{QAM}}(\gamma) = \sum_l A_l Q\left(\sqrt{a_l\gamma}\right) \tag{34}$$

where A_l and a_l are constants given in Table I.

The average BER in a specific SNR region of $[\gamma_n, \gamma_{n+1}]$ can then be computed as follows:

$$P_{n,\text{QAM}} = \int_{\gamma_n}^{\gamma_{n+1}} p_{m_n,\text{QAM}}(\gamma) p_{\gamma_{\text{ub}}}(\gamma) d\gamma \tag{35}$$

for i.i.d. Rayleigh fading for the cooperative network

$$p_{\gamma_{\text{ub}}}(\gamma) = \frac{\beta_0}{\bar{\gamma}_{s,d}} e^{-\frac{\gamma}{\bar{\gamma}_{s,d}}} + \sum_{i=1}^{m} \frac{\beta_i (0.5\bar{\gamma})^{-i}}{(i-1)!} \gamma^{i-1} e^{-\frac{\gamma}{(0.5\bar{\gamma})}}. \tag{36}$$

Substituting (34) and (36) into (35), the nth mode BER is given by

$$\begin{aligned} P_{n,\text{QAM}} &= \int_{\gamma_n}^{\gamma_{n+1}} \sum_l A_l Q\left(\sqrt{a_l\gamma}\right) \\ &\quad \times \left\{ \frac{\beta_0}{\bar{\gamma}_{s,d}} e^{-\frac{\gamma}{\bar{\gamma}_{s,d}}} + \sum_{i=1}^{m} \frac{\beta_i (0.5\bar{\gamma})^{-i}}{(i-1)!} \gamma^{i-1} e^{-\frac{\gamma}{(0.5\bar{\gamma})}} \right\} d\gamma \\ &= \frac{\beta_0}{\bar{\gamma}_{s,d}} \sum_l A_l \int_{\gamma_n}^{\gamma_{n+1}} Q(\sqrt{a_l\gamma})\, e^{-\frac{\gamma}{\bar{\gamma}_{s,d}}} d\gamma + \sum_l A_l \sum_{i=1}^{m} \frac{\beta_i (0.5\bar{\gamma})^{-i}}{(i-1)!} \\ &\quad \times \int_{\gamma_n}^{\gamma_{n+1}} Q(\sqrt{a_l\gamma})\, \gamma^{i-1} e^{-\frac{\gamma}{(0.5\bar{\gamma})}} d\gamma. \end{aligned} \tag{37}$$

Equation (37) can be solved as follows. We first define

$$I_i = \int_c^d Q\left(\sqrt{a_l\gamma}\right) \gamma^{i-1} e^{-\beta\gamma} d\gamma \tag{38}$$

$$= \int_c^d Q\left(\sqrt{a_l\gamma}\right) dF(\gamma) \tag{39}$$

$$= Q\left(\sqrt{a_l\gamma}\right) F(\gamma)\Big|_c^d - \int_c^d F(\gamma) \frac{d}{d\gamma} Q\left(\sqrt{a_l\gamma}\right) \tag{40}$$

where integration by parts is used in steps (39) and (40), and $dF(\gamma) = \gamma^{i-1}e^{-\beta\gamma}d\gamma$.

First, the cumulative distribution function is given by

$$F(\gamma) = \int_0^\gamma dF(x) = \int_0^\gamma x^{i-1}e^{-\beta x}dx \tag{41}$$

$$= \beta^{-i}\int_0^{\beta\gamma} t^{i-1}e^{-t}dt = \beta^{-i}\gamma_{\text{func}}(i, \beta\gamma) \tag{42}$$

$$= \beta^{-i}(i-1)!\left[1 - e^{-\beta\gamma}\sum_{r=0}^{i-1}\frac{(\beta\gamma)^r}{r!}\right] \tag{43}$$

where $\gamma_{\text{func}}(\alpha, x)$ is defined in [33, eqs. (8.350.1) and (8.352.1)] as

$$\gamma_{\text{func}}(\alpha, x) = \int_0^x t^{\alpha-1}e^{-t}dt$$

$$= (\alpha-1)!\left[1 - e^{-x}\sum_{r=0}^{\alpha-1}\frac{x^r}{r!}\right] \tag{44}$$

for $\alpha = 1, 2, \ldots$.

Second, using the definition

$$Q(x) = \frac{1}{\sqrt{2\pi}}\int_x^\infty \exp(-\lambda^2/2)d\lambda \tag{45}$$

we find the derivative given by

$$\frac{d}{dx}Q(x) = \frac{-\exp(-x^2/2)}{\sqrt{2\pi}}. \tag{46}$$

When $x = \sqrt{a_l\gamma} \Rightarrow dx = (\sqrt{a_l}/2)\gamma^{-0.5}d\gamma$. We obtain

$$\frac{d}{d\gamma}Q\left(\sqrt{a_l\gamma}\right) = -\frac{1}{2}\sqrt{\frac{a_l}{2\pi}}\gamma^{-0.5}\exp(-a_l\gamma/2). \tag{47}$$

By substituting (44) and (47) into (40), I_i can be written as

$$I_i = Q\left(\sqrt{a_l\gamma}\right)\beta^{-i}(i-1)!\left[1-e^{-\beta\gamma}\sum_{r=0}^{i-1}\frac{(\beta\gamma)^r}{r!}\right]\Bigg|_c^d + \frac{1}{2}\sqrt{\frac{a_l}{2\pi}}\beta^{-i}(i-1)! \times \int_c^d\left[1-e^{-\beta\gamma}\sum_{r=0}^{i-1}\frac{(\beta\gamma)^r}{r!}\right]\gamma^{-0.5}\exp(-a_l\gamma/2)d\gamma. \tag{48}$$

Now, take a look at the following:

$$\int_c^d\left[1 - e^{-\beta\gamma}\sum_{r=0}^{i-1}\frac{(\beta\gamma)^r}{r!}\right]\gamma^{-0.5}\exp(-a_l\gamma/2)d\gamma = \int_c^d \gamma^{-0.5}\exp(-a_l\gamma/2)d\gamma - \int_c^d \exp\left(-\gamma(a_l/2+\beta)\right)\sum_{r=0}^{i-1}\frac{\beta^r\gamma^{r-0.5}}{r!}d\gamma. \tag{49}$$

Furthermore, observe that

$$\int_c^d \gamma^{r-0.5}\exp(-K\gamma)d\gamma = K^{-r-0.5}\int_{cK}^{dK} t^{r-0.5}\exp(-t)dt = -K^{-r-0.5}\Gamma(r+0.5, K\gamma)\Big|_c^d \tag{50}$$

where the incomplete gamma function can be written as [33, eq. (8.350.2)]

$$\Gamma(\alpha, x) = \int_x^\infty e^{-t}t^{\alpha-1}dt. \tag{51}$$

Equation (49) can then be written as

$$= -\left(\frac{a_l}{2}\right)^{-0.5}\Gamma\left(0.5, \frac{\gamma a_l}{2}\right)\Big|_c^d + \sum_{r=0}^{i-1}\frac{\beta^r}{r!}(a_l/2+\beta)^{-r-0.5}\Gamma\left(r+0.5, (a_l/2+\beta)\gamma\right)\Big|_c^d. \tag{52}$$

Finally, I_i can be written in closed form as

$$I_i = Q\left(\sqrt{a_l\gamma}\right)\beta^{-i}(i-1)!\left[1 - e^{-\beta\gamma}\sum_{r=0}^{i-1}\frac{(\beta\gamma)^r}{r!}\right]\Bigg|_c^d - \frac{1}{2}\beta^{-i}(i-1)!\Bigg\{(\pi)^{-0.5}\Gamma(0.5, \frac{\gamma a_l}{2})\Big|_c^d - \sqrt{\frac{a_l}{2\pi}}\sum_{r=0}^{i-1}\frac{\beta^r}{r!}(a_l/2+\beta)^{-r-0.5} \times \Gamma(r+0.5, (a_l/2+\beta)\gamma)\Big|_c^d\Bigg\}. \tag{53}$$

Also, we are interested in I_1, which is given by

$$I_1 = Q(\sqrt{a_l\gamma})\beta^{-1}[1 - e^{-\beta\gamma}]\Big|_c^d - \frac{1}{2}\beta^{-1}\Bigg\{(\pi)^{-0.5}\Gamma\left(0.5, \frac{\gamma a_l}{2}\right)\Big|_c^d - \sqrt{\frac{a_l}{2\pi}}(a_l/2+\beta)^{-0.5}\Gamma(0.5, (a_l/2+\beta)\gamma)\Big|_c^d\Bigg\}. \tag{54}$$

Last, the average BER of (37) can be written as follows by substituting I_1 and I_i:

$$
\begin{aligned}
P_{n,\mathrm{QAM}} &= \beta_0 \sum_l A_l \Bigg[Q\left(\sqrt{a_l\gamma}\right)\left[1-e^{-\frac{\gamma}{\bar{\gamma}_{s,d}}}\right]\Bigg|_{\gamma_n}^{\gamma_{n+1}} \\
&\quad - \frac{1}{2}\Bigg\{ (\pi)^{-0.5}\Gamma\left(0.5, \frac{\gamma a_l}{2}\right)\Bigg|_{\gamma_n}^{\gamma_{n+1}} \\
&\quad - \sqrt{\frac{a_l}{2\pi}}\left(a_l/2+\bar{\gamma}_{s,d}^{-1}\right)^{-0.5} \\
&\quad \times \Gamma\left(0.5, \left(a_l/2+\bar{\gamma}_{s,d}^{-1}\right)\gamma\right)\Bigg|_{\gamma_n}^{\gamma_{n+1}} \Bigg\}\Bigg] \\
&\quad + \sum_l A_l \sum_{i=1}^{m} \beta_i \\
&\quad \times \Bigg[Q\left(\sqrt{a_l\gamma}\right)\left(1-e^{-\frac{\gamma}{(0.5\bar{\gamma})}}\sum_{r=0}^{i-1}\frac{(2\gamma/\bar{\gamma})^r}{r!}\right)\Bigg|_{\gamma_n}^{\gamma_{n+1}} \\
&\quad - \frac{1}{2}\Bigg\{ (\pi)^{-0.5}\Gamma\left(0.5, \frac{\gamma a_l}{2}\right)\Bigg|_{\gamma_n}^{\gamma_{n+1}} \\
&\quad - \sqrt{\frac{a_l}{2\pi}}\sum_{r=0}^{i-1}\frac{(0.5\bar{\gamma})^{-r}}{r!}(a_l/2+2/\bar{\gamma})^{-r-0.5} \\
&\quad \times \Gamma\left(r+0.5, (a_l/2+2/\bar{\gamma})\gamma\right)\Bigg|_{\gamma_n}^{\gamma_{n+1}} \Bigg\}\Bigg]. \qquad (55)
\end{aligned}
$$

Case of Non-I.I.D. Fading Channels: In a similar fashion as the i.i.d. case and by using the non-i.i.d. pdf

$$
p_{\gamma_{\mathrm{ub}}}(\gamma) = \frac{\widehat{\beta}_0}{\bar{\gamma}_{s,d}} e^{-\frac{\gamma}{\bar{\gamma}_{s,d}}} + \sum_{i=1}^{m}\frac{\widehat{\beta}_i}{\tau_i}e^{-\frac{\gamma}{\tau_i}} \qquad (56)
$$

and substituting (34) and (56) into (35), we obtain the nth mode BER as follows:

$$
\begin{aligned}
P_{n,QAM} &= \int_{\gamma_n}^{\gamma_{n+1}} \sum_l A_l Q\left(\sqrt{a_l\gamma}\right) \\
&\quad \times \left\{ \frac{\widehat{\beta}_0}{\bar{\gamma}_{s,d}} e^{-\frac{\gamma}{\bar{\gamma}_{s,d}}} + \sum_{i=1}^{m}\frac{\widehat{\beta}_i}{\tau_i}e^{-\frac{\gamma}{\tau_i}} \right\} d\gamma. \qquad (57)
\end{aligned}
$$

Equation (57) can be rearranged as

$$
\begin{aligned}
P_{n,\mathrm{QAM}} &= \frac{\widehat{\beta}_0}{\bar{\gamma}_{s,d}} \sum_l A_l \int_{\gamma_n}^{\gamma_{n+1}} Q\left(\sqrt{a_l\gamma}\right) e^{-\frac{\gamma}{\bar{\gamma}_{s,d}}} d\gamma \\
&\quad + \sum_l A_l \sum_{i=1}^{m} \frac{\widehat{\beta}_i}{\tau_i} \int_{\gamma_n}^{\gamma_{n+1}} Q\left(\sqrt{a_l\gamma}\right) e^{-\frac{\gamma}{\tau_i}} d\gamma. \qquad (58)
\end{aligned}
$$

Substituting I_1 in (54) into (58), we find

$$
\begin{aligned}
P_{n,\mathrm{QAM}} &= \widehat{\beta}_0 \sum_l A_l \Bigg[Q(\sqrt{a_l\gamma})\Big[1-e^{-\frac{\gamma}{\bar{\gamma}_{s,d}}}\Big]\Bigg|_{\gamma_n}^{\gamma_{n+1}} \\
&\quad - \frac{1}{2}\Bigg\{ (\pi)^{-0.5}\Gamma\Big(0.5, \frac{\gamma a_l}{2}\Big)\Bigg|_{\gamma_n}^{\gamma_{n+1}} \\
&\quad - \sqrt{\frac{a_l}{2\pi}}\left(a_l/2+\bar{\gamma}_{s,d}^{-1}\right)^{-0.5} \\
&\quad \times \Gamma\left(0.5, \left(a_l/2+\bar{\gamma}_{s,d}^{-1}\right)\gamma\right)\Bigg|_{\gamma_n}^{\gamma_{n+1}} \Bigg\}\Bigg] \\
&\quad + \sum_l A_l \sum_{i=1}^{m} \widehat{\beta}_i \Bigg[Q(\sqrt{a_l\gamma})\Big[1-e^{-\frac{\gamma}{\tau_i}}\Big]\Bigg|_{\gamma_n}^{\gamma_{n+1}} \\
&\quad - \frac{1}{2}\Bigg\{ (\pi)^{-0.5}\Gamma\Big(0.5, \frac{\gamma a_l}{2}\Big)\Bigg|_{\gamma_n}^{\gamma_{n+1}} \\
&\quad - \sqrt{\frac{a_l}{2\pi}}\left(a_l/2+\tau_i^{-1}\right)^{-0.5} \\
&\quad \times \Gamma\big(0.5, \left(a_l/2+\tau_i^{-1}\right)\gamma\big)\Bigg|_{\gamma_n}^{\gamma_{n+1}} \Bigg\}\Bigg]. \qquad (59)
\end{aligned}
$$

ACKNOWLEDGMENT

The authors would like to thank K. Phan of the University of Alberta, Edmonton, AB, Canada, and H. Nguyen of the University of Saskatchewan, Saskatoon, SK, Canada, for their contributions to the previous work [27], [28], which inevitably led to this paper.

REFERENCES

[1] A. J. Goldsmith and P. P. Varaiya, "Capacity of fading channels with channel side information," *IEEE Trans. Inf. Theory*, vol. 43, no. 6, pp. 1986–1992, Nov. 1997.

[2] M.-S. Alouini and A. J. Goldsmith, "Capacity of Rayleigh fading channels under different adaptive transmission and diversity-combining techniques," *IEEE Trans. Veh. Technol.*, vol. 48, no. 4, pp. 1165–1181, Jul. 1999.

[3] A. J. Goldsmith and S.-G. Chua, "Variable-rate variable-power MQAM for fading channels," *IEEE Trans. Commun.*, vol. 45, no. 10, pp. 1218–1230, Oct. 1997.

[4] M.-S. Alouini and A. J. Goldsmith, "Adaptive modulation over Nakagami fading channels," *Wirel. Pers. Commun.*, vol. 13, no. 1/2, pp. 119–143, May 2000.

[5] R. K. Mallik, M. Z. Win, M.-S. Alouini, and A. J. Goldsmith, "Channel capacity of adaptive transmission with maximal ratio combining in correlated Rayleigh fading," *IEEE Trans. Wireless Commun.*, vol. 3, no. 4, pp. 1124–1133, Jul. 2004.

[6] A. Sendonaris, E. Erkip, and B. Aazhang, "User cooperation diversity—Part I: System description," *IEEE Trans. Commun.*, vol. 51, no. 11, pp. 1927–1938, Nov. 2003.

[7] J. N. Laneman, D. N. C. Tse, and G. W. Wornell, "Cooperative diversity in wireless networks: Efficient protocols and outage behavior," *IEEE Trans. Inf. Theory*, vol. 50, no. 12, pp. 3062–3080, Dec. 2004.

[8] M. O. Hasna and M.-S. Alouini, "End-to-end performance of transmission systems with relays over Rayleigh-fading channels," *IEEE Trans. Wireless Commun.*, vol. 2, no. 6, pp. 1126–1131, Nov. 2003.

[9] S. Ikki and M. H. Ahmed, "Performance analysis of cooperative diversity wireless networks over Nakagami-m fading channel," *IEEE Commun. Lett.*, vol. 11, no. 4, pp. 334–336, Apr. 2007.

[10] A. S. Avestimehr and D. N. C. Tse, "Outage capacity of the fading relay channel in the low-SNR regime," *IEEE Trans. Inf. Theory*, vol. 53, no. 4, pp. 1401–1415, Apr. 2007.

[11] N. C. Beaulieu and J. Hu, "A closed-form expression for the outage probability of decode-and-forward relaying in dissimilar Rayleigh fading channels," *IEEE Commun. Lett.*, vol. 10, no. 12, pp. 813–815, Dec. 2006.

[12] H. A. Suraweera, P. J. Smith, and J. Armstrong, "Outage probability of cooperative relay networks in Nakagami-m fading channels," *IEEE Commun. Lett.*, vol. 10, no. 12, pp. 834–836, Dec. 2006.

[13] L. Le and E. Hossain, "An analytical model for ARQ cooperative diversity in multi-hop wireless networks," *IEEE Trans. Wireless Commun.*, vol. 7, no. 5, pp. 1786–1791, May 2008.

[14] O. Canpolat, M. Uysal, and M. M. Fareed, "Analysis and design of distributed space-time trellis codes with amplify-and-forward relaying," *IEEE Trans. Veh. Technol.*, vol. 56, no. 4, pp. 1649–1660, Jul. 2007.

[15] S. Yiu, R. Schober, and L. Lampe, "Distributed space-time block coding," *IEEE Trans. Commun.*, vol. 54, no. 7, pp. 1195–1206, Jul. 2006.

[16] C. H. Cho, K. T. Kim, and H. Y. Youn, "Mobile multi-hop relay system using AMC for multicast broadcast service over mobile WiMAX," in *Proc. WTS*, Pomona, CA, Apr. 2008, pp. 46–52.

[17] B. Can, H. Yanikomeroglu, F. A. Onat, E. De Carvalho, and H. Yomo, "PHY 02-2—Efficient cooperative diversity schemes and radio resource allocation for IEEE 802.16j," in *Proc. IEEE WCNC*, Las Vegas, NV, Mar./Apr. 2008, pp. 36–41.

[18] A. Host-Madsen and J. Zhang, "Capacity bounds and power allocation for wireless relay channels," *IEEE Trans. Inf. Theory*, vol. 51, no. 6, pp. 2020–2040, Jun. 2005.

[19] Y. Liang and V. V. Veeravalli, "Resource allocation for wireless relay channels," in *Proc. 38th Asilomar Conf. Signals, Syst., Comput.*, Nov. 2004, vol. 2, pp. 1902–1906.

[20] D. Gunduz and E. Erkip, "Opportunistic cooperation by dynamic resource allocation," *IEEE Trans. Wireless Commun.*, vol. 6, no. 4, pp. 1446–1454, Apr. 2007.

[21] O. Kaya and S. Ulukus, "Power control for fading multiple access channels with user cooperation," in *Proc. Int. Conf. Wireless Netw., Commun. Mobile Comput.*, Jun. 2005, vol. 2, pp. 1443–1448.

[22] D. S. Michalopoulos and G. K. Karagiannidis, "PHY-layer fairness in amplify and forward cooperative diversity systems," *IEEE Trans. Wireless Commun.*, vol. 7, no. 3, pp. 1073–1082, Mar. 2008.

[23] Y. Zhao, R. Adve, and T. J. Lim, "Improving amplify-and-forward relay networks: Optimal power allocation versus selection," *IEEE Trans. Wireless Commun.*, vol. 6, no. 8, pp. 3114–3123, Aug. 2007.

[24] C. T. K. Ng and A. J. Goldsmith, *The impact of CSI and power allocation on relay channel capacity and cooperation strategies*, 2007. [Online]. Available: http://www.citebase.org/abstract?id=oai:arXiv.org:cs/0701116

[25] B. Choi and L. Hanzo, "Optimum mode-switching-assisted constant-power single- and multicarrier adaptive modulation," *IEEE Trans. Veh. Technol.*, vol. 52, no. 3, pp. 536–560, May 2003.

[26] M. O. Hasna, "On the capacity of cooperative diversity systems with adaptive modulation," in *Proc. 2nd IFIP Int. Conf. WOCN*, Mar. 2005, pp. 432–436.

[27] T. Nechiporenko, K. Phan, C. Tellambura, and H. H. Nguyen, "On the capacity of Rayleigh fading cooperative systems under adaptive transmission," *IEEE Trans. Wireless Commun.*. : Accepted for future publication.

[28] T. Nechiporenko, K. T. Phan, C. Tellambura, and H. H. Nguyen, "Performance analysis of adaptive M-QAM for Rayleigh fading cooperative systems," in *Proc. IEEE ICC*, May 2008, pp. 3393–3399.

[29] K. S. Hwang, Y. Ko, and M.-S. Alouini, "Performance analysis of opportunistic incremental relaying with adaptive modulation over cooperative networks," in *Proc. IEEE Int. Symp. Wireless Pervasive Comput.*, May 2008, pp. 586–590.

[30] P. A. Anghel and M. Kaveh, "Exact symbol error probability of a cooperative network in a Rayleigh-fading environment," *IEEE Trans. Wireless Commun.*, vol. 3, no. 5, pp. 1416–1421, Sep. 2004.

[31] J. Park and C. H. Lim, "An adaptive modulation scheme with switched diversity for Rayleigh fading channels," in *Proc. APCC*, Busan, Korea, Aug. 2006, pp. 1–4.

[32] Z. Katona and J. Bito, "Performance analysis of cross layer adaptation of modulation and coding in slow, flat fading channels," in *Proc. 16th IST Mobile Wireless Commun. Summit*, Budapest, Hungary, Jul. 2007, pp. 1–5.

[33] I. Gradshteyn and I. Ryzhik, *Table of Integrals, Series, and Products*, 6th ed. New York: Academic, 2000.

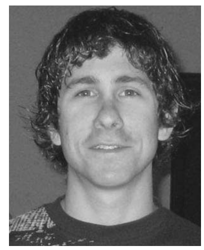

Tyler Nechiporenko (S'02) received the B.Sc. degrees in electrical engineering and in computer science from the University of Saskatchewan, Saskatoon, SK, Canada, in 2007 and the M.Sc. degree in electrical engineering from the University of Alberta, Edmonton, AB, Canada, in 2008.

In the summers of 2004 and 2007, he was with the Department of Electrical and Computer Engineering, University of Saskatchewan, sponsored by the Natural Sciences and Engineering Research Council of Canada (NSERC) Undergraduate Student Research Award. In 2005 and 2006, he was with SED Systems as an Intern with the Hardware Engineering—Digital Design Group. He is currently with the University of Alberta. His research interests include the wide area of wireless communications.

Mr. Nechiporenko was a recipient of the NSERC Canada Graduate Scholarship and the Informatics Circle of Research Excellence Graduate Student Scholarship in 2007 and 2008.

Prasanna Kalansuriya (S'08) received the B.Sc. degree (with First-Class Honors) from the University of Moratuwa, Moratuwa, Sri Lanka, in 2005. He is currently working toward the M.Sc. degree with the Department of Electrical and Computer Engineering, University of Alberta, Edmonton, AB, Canada.

His research interests include cooperative diversity and adaptive transmission.

Chintha Tellambura (SM'02) received the B.Sc. degree (with First-Class Honors) from the University of Moratuwa, Moratuwa, Sri Lanka, in 1986, the M.Sc. degree in electronics from the University of London, London, U.K., in 1988, and the Ph.D. degree in electrical engineering from the University of Victoria, Victoria, BC, Canada, in 1993.

In 1993 and 1994, he was a Postdoctoral Research Fellow with the University of Victoria and, in 1995 and 1996, with the University of Bradford, Bradford, U.K. From 1997 to 2002, he was with Monash University, Melbourne, Australia. He is currently a Professor with the Department of Electrical and Computer Engineering, University of Alberta, Edmonton, AB, Canada. His research interests include diversity and fading countermeasures, multiple-input–multiple-output systems and space–time coding, and orthogonal frequency-division multiplexing.

Prof. Tellambura is an Associate Editor for the IEEE TRANSACTIONS ON COMMUNICATIONS and the Area Editor for Wireless Communications Systems and Theory for the IEEE TRANSACTIONS ON WIRELESS COMMUNICATIONS. He was the Chair of the Communication Theory Symposium in IEEE Global Telecommunications Conference 2005, St. Louis, MO.